Effect of Annealing on Electrical Conductivity and Morphology of Polyaniline Films

ANURAG LODHA, S. MICHAEL KILBEY II, PRAVEEN C. RAMAMURTHY, RICHARD V. GREGORY

[1] Department of Chemical Engineering, Clemson University, Clemson, South Carolina 29634

[2] School of Textiles, Fibers and Polymer Science, Clemson University, Clemson, South Carolina 29634

Received 25 July 2000; accepted 1 May 2001

ABSTRACT: We report structure–property relationships of polyaniline emeraldine base (EB) films that were produced by combining different processing steps in various sequences. The effect of annealing and doping processes on the surface structure of the films was investigated by atomic force microscopy (AFM), and the corresponding changes to the chemical structure of the EB films were monitored by Fourier transform infrared spectroscopy. AFM results indicate that after doping polyaniline (EB) films with HCl, the root mean square (rms) roughness of the surface of EB film increased ~ 46%. When the doped films were annealed at 180°C under a nitrogen atmosphere for 3 h, the rms roughness was essentially unchanged from that of the initial, undoped films. The electrical conductivity of the films also showed a significant dependence on the processing sequence. When the doped polyaniline (EB) films were annealed, no electrical conductivity was observed. When these films were redoped, only ~ 6% of the initial conductivity could be recovered. In another processing sequence in which the polyaniline (EB) films were first annealed and then doped, the electrical conductivity was only ~ 12% relative to the film that was doped immediately after being cast. From this work, a strategy to reduce the surface roughness of films made from electrically conducting polyaniline (EB) is proposed. © 2001 John Wiley & Sons, Inc. J Appl Polym Sci 82: 3602–3610, 2001

Key words: polyaniline films; annealing; surface roughness; electrical conductivity

INTRODUCTION

There is considerable interest in using electrically conducting polymers (CPs) in microelectronics because CPs are flexible, possess a high strength-to-weight ratio, and are relatively cheap compared with silicon. It has been suggested that it is possible to process CPs on mass scales by techniques such as ink-jet printing and screen printing, which offers an opportunity for low-cost manufacturing of polymer-based, electronic devices, such as heterojunction diodes and thin film transistors (TFTs).[1,2]

The first successful attempt to fabricate a polymer-based heterojunction diode and TFT was made by Ebisawa and co-workers[3] in 1983. Since then, various research groups have used a variety of CPs to fabricate heterojunction devices and TFTs. Despite substantial advances in the last 10 years in materials and processing techniques, the performance of devices based on CPs remains inferior to inorganic devices. The most important concern associated with the performance of the polymer-based devices is that high voltages are needed to operate the devices. A high-power re-

Correspondence to: S. Michael Kilbey II (mike.kilbey@ces.clemson.edu).

Journal of Applied Polymer Science, Vol. 82, 3602–3610 (2001)

quirement is not desirable for lightweight and portable devices because a large power draw would quickly drain a portable power source, such as a battery.[4–7] Typically, high voltages are required to operate the polymer-based devices because of inefficient charge transport properties at the interface between the CP and metal electrode. Therefore, making intimate contact between the CP and metal electrode is crucial when fabricating heterojunction diodes and TFTs. Minimizing the surface roughness is one way to achieve intimate contact between the CP and metal electrode and also improve device performance.

Depending on the degree of interfacial roughness, there may be defects or small spikes at the interface, which lead to a nonuniform electric field at the interface. If the spike is large enough, it can cause failure of the device because of short-circuits induced by tunneling effects. In any case, the performance of such a device will not be reliable.[8] Hence, the roughness at the surface of the polymer is one of the most significant parameters that affect the performance of polymer-based diodes and TFTs.[9]

One parameter that can be used to quantify the performance characteristics of a heterojunction diode is the ideality factor, which represents the nature of contact between the CP and metal electrode. In the case of Schottky diodes, the ideality factor indicates the uniformity of the interface between polymer and metal electrode. For an ideal Schottky barrier, the ideality factor is unity.[10] In Schottky diodes, high ideality factors occur because of inefficient transport of charge carriers due to variations in thickness and nonuniform interfacial charges, which result in locally defective hot regions.[9–12]

Another important concern with using CPs in devices is that they are unstable when exposed to ambient conditions. For example, polymers that behave as *n*-type materials after doping, oxidize when exposed to the atmosphere.[13,14] As a result, devices made from these CPs would not be reliable for practical applications because their performance would not be consistent. One reason polyaniline is of great interest is because it has better thermal and environmental stability compared with other CPs.[15–21] Therefore, polyaniline is a promising material for fabricating electronic devices, such as heterojunction diodes and TFTs.[10,22] Although polyaniline was first synthesized in 1862 and has been studied as an electrically conducting polymer since the 1980s,[23,24] the performance of polyaniline-based diodes and TFTs is relatively poor when compared with other CPs.[10,12] Though it is known that the nature of the interface between the CP and metal electrode has a significant impact on the device performance, little work has been done to understand the factors that control surface roughness and to design processes that minimize the roughness of the polyaniline emeraldine base (EB) films. In this paper, the possibility of adapting doping and thermal treatment processes to improve the morphology and electrical properties of polyaniline films will be examined in detail.

EXPERIMENTAL

Synthesis of Polyaniline

Polyaniline powder in the form of emeraldine base (EB) was synthesized by chemical oxidation in an acidic solution. Prior to polymerization, aniline was mixed in 1 M HCl. The freezing temperature of the solution was reduced below the synthesis temperature by adding a 6 M LiCl solution using a procedure similar to that reported by Angelopoulos et al.[25] This aniline solution was kept in a Cryocool immersion cooler with isopropanol as the cooling agent. Ammonium persulfate (APS) dissolved in dionized water was used as the oxidant. Polymerization was initiated when the temperature of aniline solution was -40°C by adding APS in a dropwise manner at a rate of 5 mL/min. The molar ratio of aniline to APS in the reaction mixture was 1 : 1. Polymerization was carried out for 48 h under a nitrogen atmosphere. The reaction mixture was continuously stirred during polymerization and, in the course of the reaction, the color of the mixture turned from pink to copper to dark blue. After polymerization, the dark-blue precipitate was filtered and washed with deionized water and methanol until the color of the wash solution was light violet. The powder was de-doped by stirring it in a solution of 0.1 M ammonium hydroxide for 18 h. The resulting mixture was filtered by vacuum filtration and washed repeatedly with deionized water to obtain the EB powder.

The EB powder was washed with distilled water and methanol until the wash solution was colorless. Using a Soxhlet Extraction method with methanol as the solvent, oligomers and low molecular weight polymer were removed over a period of 5 days (recharging methanol every 12 h) until the extracted solution became a light violet

color. The purified EB powder was dried under vacuum (26 mmHg) at 50°C for 24 h. The Fourier transform infrared (FTIR) analysis of the EB powder was in excellent agreement with the chemical structure as reported in the literature.[16,23,26,27] Molecular weight was determined by gel permeation chromatography using *N*-methyl-2-pyrrolidinone (NMP) solvent (Aldrich, used as received) and polystyrene standards. The weight-average molecular weight (M_w) based on the polystyrene standards was 30,000 g mol^{-1}.

Film Preparation

Polyaniline (EB) solution (3.5 wt % EB) was prepared at room temperature by dissolving the EB powder in *N*,*N*′-diemthyl propylene urea (DMPU; Aldrich, used as received). The EB powder was added very slowly into the solvent over a period of 1 week to avoid gelation. The polyaniline (EB) solution was then filtered through a 25-μm filter to remove any undissolved and shear-induced agglomerates.[25] This solution was used to prepare free-standing films. The free-standing films were made by pouring small quantities of the polyaniline (EB) solution onto specimen slides (Sigma, used as received). The slides were then placed in a vacuum oven under a vacuum of 15 mmHg at 60°C to remove the solvent by evaporation. After drying for 24 h, these films were immersed in a water bath for 30 min to float the films off the specimen slides. The films were then dried on a filter paper and stored in a sealed container. The films were doped by a film immersion technique.[21,28] The films to be doped were immersed in a 1 M HCl solution for 48 h and kept in a closed chamber at room temperature. The doped films were then removed and dried on filter paper and stored in a sealed container.

The polyaniline (EB) films were annealed below the cross-linking temperature, which had been determined by thermogravimetric analysis (TGA) and differential scanning calorimetry (DSC). These measurements indicated the cross-linking temperature was ~ 200°C, which is consistent with the observations of Ding et al.[16] Thus, an annealing temperature of 180°C was selected to avoid cross-linking. The films were placed in an oven and heated at the rate of 10°C/min to 180°C under a nitrogen atmosphere. The temperature was held at 180°C for 3 h, after which the films were allowed to cool naturally in the nitrogen environment. The films were heated at the rate of 10°C/min. so that the conditions for different experiments, such as TGA and DSC, would be identical. Four sets of samples—undoped, doped, annealed and then doped, doped and then annealed—were made.

For ease of reference, the following nomenclature has been adopted in this paper: *U* = undoped, *D* = doped, *A* = annealed, and *R* = redoped. A string of these letters indicates both the processes and the sequence of steps the films have undergone. For example, a film referred to as *UAD* would imply that the undoped EB film was first annealed and then doped. Similarly, a film identified by *UDAR* means that the undoped film was first doped, then annealed, and finally redoped. The final letter in the string always indicates the final condition of the film.

Film Characterization

TGA experiments were carried out using a TA Instruments Hi-Res Thermogravimetric Analyzer (model 2950). A known weight of the polyaniline (EB) film was heated at the rate of 10°C/min under a nitrogen atmosphere. DSC was carried out under a nitrogen atmosphere using a TA Instruments model 2920. A heating rate of 10°C/min was used to heat the samples from room temperature to 400°C. The FTIR spectra of the EB films were observed using diffuse reflectance mode on a using a Nicolet Magna 550 FTIR spectrophotometer. Samples were scanned in the range 4000–400 cm^{-1}, and the scan resolution was 4 cm^{-1}. For each sample, 64 scans were taken. The data were collected using a DTgS infrared detector. The electrical conductivity of the films was determined by using the standard four-point probe technique with a Keithley 2000 programmable multimeter. The root mean square (rms) roughness of the films after various processing steps was determined using a Digital Instruments, Nanoscope III AFM/STM in tapping mode. The rms values consider the entire film surface. Measurements were made using a standard silicon-nitride tip.

RESULTS AND DISCUSSION

A TGA thermogram of a free-standing, *U* polyaniline (EB) film taken in nitrogen atmosphere is shown in Figure 1. Two distinct stages of weight loss were observed. An initial weight loss of ~ 15% was observed over a range 100–250°C. This result is attributed to loss of moisture, low

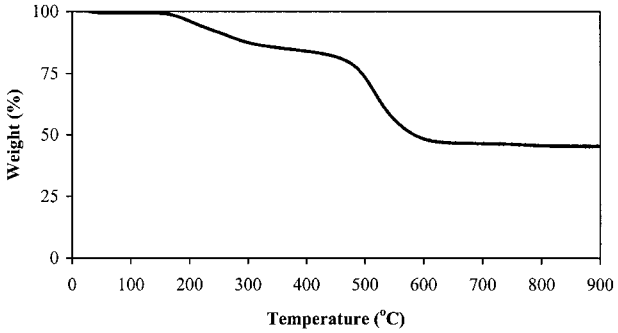

Figure 1 Typical TGA thermogram of an undoped polyaniline (EB) film in a nitrogen atmosphere. The heating rate was 10°C/min.

molecular weight oligomers, and residual solvent, and is consistent with previous reports by other groups.[15,18] The second weight loss of ~ 40% indicated that EB films begin to degrade at 300°C and are completely decomposed at 630°C. Similar trends for weight losses associated with polyaniline (EB) films and powder have been reported, however the temperature at which the different stages of weight loss occurs are different.[27,29] This difference is most likely due to variations in the sample preparation methods and solvents used. Wei et al.[21] reported that there was only one weight loss at ~ 400°C when the films did not contain any solvent. For their EB film, which was made by free-casting of EB dissolved in NMP, there was a 16% weight loss in the range 50–270°C and a weight loss of ~ 30% at ~ 500°C. The first stage of weight loss was due to evaporation of NMP solvent and moisture. The second major weight loss was attributed to structural decomposition of the polyaniline.

The DSC thermogram for the *U* polyaniline (EB) film is shown in Figure 2. An endothermic peak is observed between 65 and 115°C, followed by two broad, exothermic peaks at 180–270 and 300–380°C. The endothermic peak indicates removal of moisture and solvent and is consistent with the corresponding weight loss shown in the TGA thermogram. Similar observations have been made by Abell et al.,[15] Paul et al.,[18] and Wei et al.[21] As reported by Ding et al.,[16] the first exothermic peak is related to cross-linking and reorientation of the polyaniline chains. There is no decomposition in the temperature range of the first exotherm because no corresponding weight loss is observed in the TGA thermogram. However, the second broad exothermic peak between 300 and 380°C is attributed to structural decomposition and/or partial degradation of the EB films. This observation is supported by the corresponding significant weight loss indicated in the TGA thermogram in this temperature range. Based on the TGA and DSC results, the EB films were annealed at 180°C, which appeared to be below the temperature at which there is a substantial change in the polyaniline (EB) films. However, as the experimental results will show, annealing at 180°C is too close to the temperature at which polyaniline (EB) films start to cross-link. Although wide angle X-ray studies were consistent with those reported by other groups, further studies are being conducted to understand the influence of annealing on the polyaniline (EB) structure in the films near the temperature range at which cross-linking is observed.

The chemical structure of a polymer chain can be identified with the help of a FTIR analysis of the polymer sample. The quinoid and benzoid rings shown in Figure 3 form the backbone of polyaniline (EB). As indicated by the figure, the conversion of quinoid rings to benzoid rings due to protonation results in the formation of charge carriers along the polymer chain. Therefore, the presence of quinoid rings in polyaniline (EB) before doping is critical to achieving any electrical conductivity. The conversion of quinoid rings to benzoid rings that occurs during annealing has a significant impact on the electrical conductivity of the films; this conversion results in fewer doping sites available for protonation and, therefore, a decrease in the electrical conductivity of the films due to lack of significant polaron formation.[27]

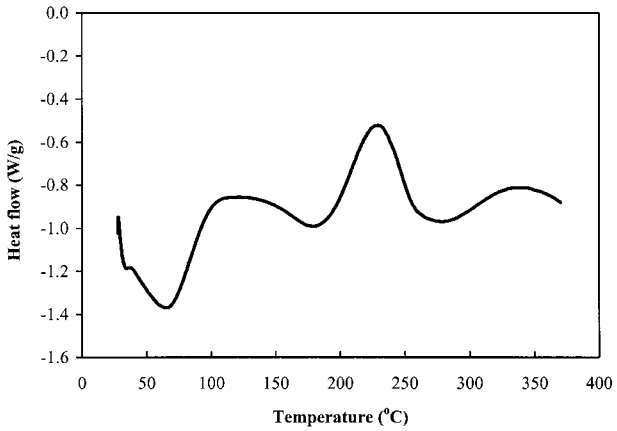

Figure 2 Conventional DSC thermogram of an undoped polyaniline (EB) film in a nitrogen atmosphere. The heating rate was 10°C/min and exothermic is "up" from the initial starting point of the trace.

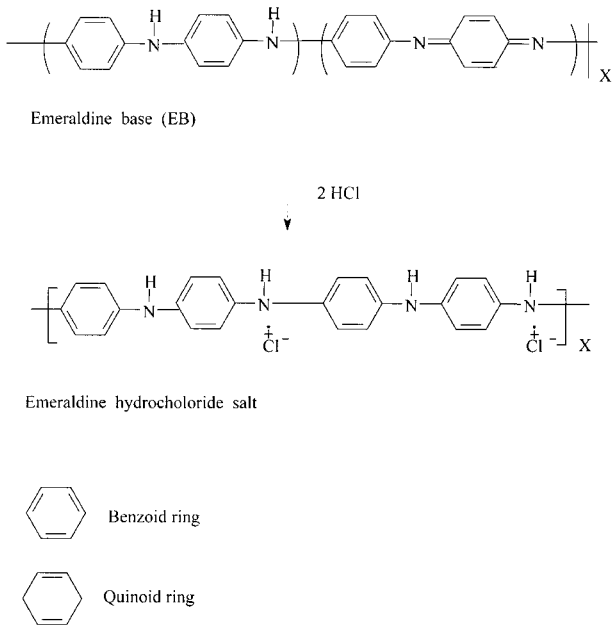

Figure 3 Protonation of polyaniline (EB) converts the emeraldine base to emeraldine hydrochloride salt, which is the conducing form of polyaniline. This reaction also shows that the presence of quinoid structures in the polymer chain is significant because they are the doping sites.

The FTIR spectra of the films shown in Figure 4 were recorded after processing the films under different conditions. The ratio of the peaks at $\sim$ 1530 and $\sim$ 1615 cm^{-1} can be compared to assess the relative amount of benzoid ($\sim$ 1530 cm^{-1}) and quinoid ($\sim$ 1615 cm^{-1}) rings in the EB samples. As previously reported by Ding et al.,[16] an increase in the ratio of the intensities at $\sim$ 1530 cm^{-1} (benzoid rings) to $\sim$ 1615 cm^{-1} (quinoid rings), I_{1530}/I_{1615}, signifies the conversion of quinoid rings to benzoid rings during the annealing process. The ratio of these peaks in the FTIR spectrum of the *U* polyaniline (EB) film

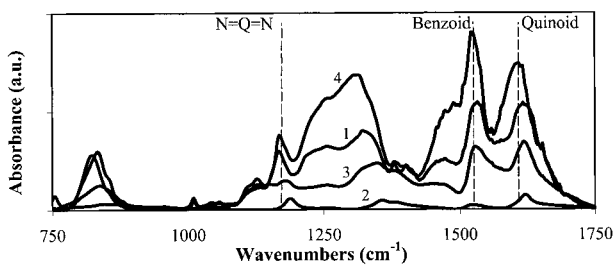

Figure 4 FTIR spectra of polyaniline (EB) films (1) *U*, (2) *UD*, (3) *UDA*, and (4) *UA*. These films were 53.9 $\pm$ 3.8 μm in thickness.

Table I Electrical Conductivity of the Polyaniline (EB) Films Processed under Different Conditions

EB Films after Various Processing Steps[a]	Electrical Conductivity (S/cm)	Normalized Ratio (%)
U	$< 10^{-10}$	—
D	0.144 $\pm$ 0.009	100.0
DA	$< 10^{-10}$	0.0
DAR	0.008 $\pm$ 0.001	5.6
UA	$< 10^{-10}$	0.0
UAD	0.017 $\pm$ 0.001	11.8

[a] The films were 53.9 $\pm$ 3.8 μm thick.

(shown as curve '1' in Figure 4) and that of the *UDA* film (shown as curve '3' in Figure 4) are approximately the same; this result indicates that the relative amount of benzoid and quinoid structure in these two samples is the same. The FTIR spectrum of the *UA* polyaniline (EB) film (shown as curve '4' in Figure 4) shows a relative increase in the intensity of the peak at $\sim$ 1530 cm^{-1} and a relative decrease in the intensity of the peak at $\sim$ 1615 cm^{-1} compared to the *U* film (shown as curve '1' in Figure 4). Similar observations were also made by Tang et al.[23] and Cao et al.[26] It is not clear if this conversion occurs as a result of some cross-linking at the imine nitrogen of the quinoid ring with another imine nitrogen, or cross-linking with an amine nitrogen within the polymer chain or on a neighboring polymer chain. It should be noted that the temperature at which the films were annealed, 180°C, was selected because it appeared to be below the temperature at which cross-linking was seen in the DSC experiments. Nevertheless, the presence of the peak at $\sim$ 1615 cm^{-1} in the FTIR spectra of the *UA* film, identified as '4' in Figure 4, clearly shows that after annealing at 180°C there is a substantial amount of quinoid rings present in the polymer chain. The presence of quinoid rings is also evidenced by the fact that after doping this *UA* polyaniline (EB) film, the *UAD* film shows some electrical conductivity. This topic will be revisited later in this paper.

The electrical conductivity of the polyaniline (EB) films after different processing steps is shown in Table I. Also shown in Table I is a normalized comparison of the electrical conductivity; the initial conductivity of the films was assumed to be 100% and the electrical conductiv-

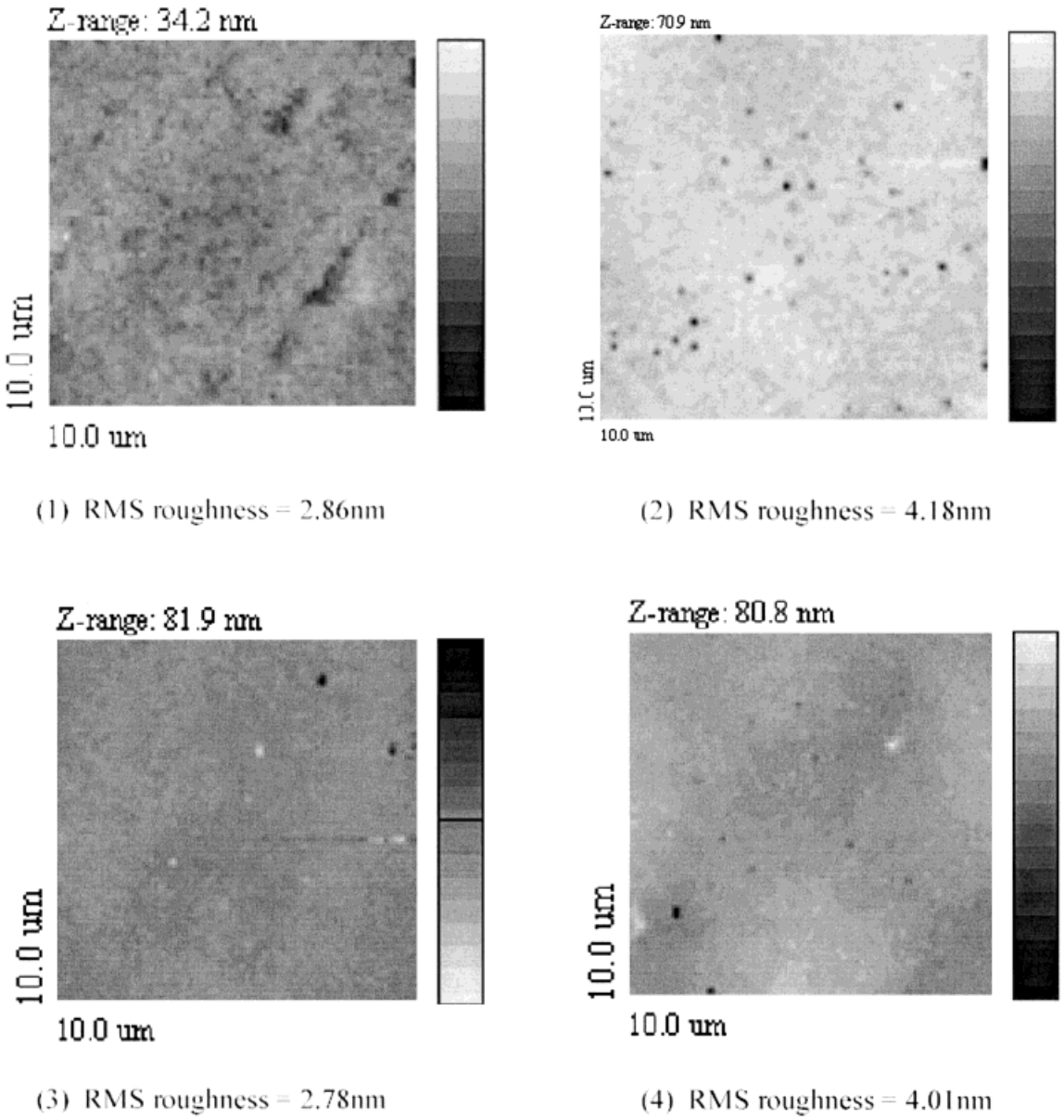

Figure 5 AFM images of EB films (1) *U*, (2) *UD*, (3) *UDA*, and (4) *UA*. The graded bar scale to the right of the AFM image indicates the feature depth, with the darkest shade representing the deepest point. Note: this scale is reversed for sample (2) to provide a clear picture.

ity of the processed films was calculated as a normalized percentage of that initial conductivity. The electrical conductivity of the film that was doped immediately after being cast, *UD*, was 0.144 ± 0.009 S/cm (100%). Essentially no electrical conductivity was observed after annealing this film (*UDA*) in nitrogen atmosphere at 180°C for 3 h. Annealing at a high temperature, such as 180°C, results in a greater amount of dopant diffusion from the films,[30] and therefore, no electrical conductivity was observed in these films after annealing.

As shown in the FTIR spectra in Figure 4, the ratio of the intensities of the peaks at ~ 1530 and ~ 1615 cm^{-1}, which indicates the relative amount of benzoid and quinoid structures, is approximately the same for the *U* films (curve '1') and the *UDA* films (curve '3'). Based on this result we anticipated that the electrical conductivity of the *UDA* films could be completely recovered on redoping. Ansari et al.[30] found that ~ 80% of the original electrical conductivity of the polyaniline (EB) films that were annealed in both air and

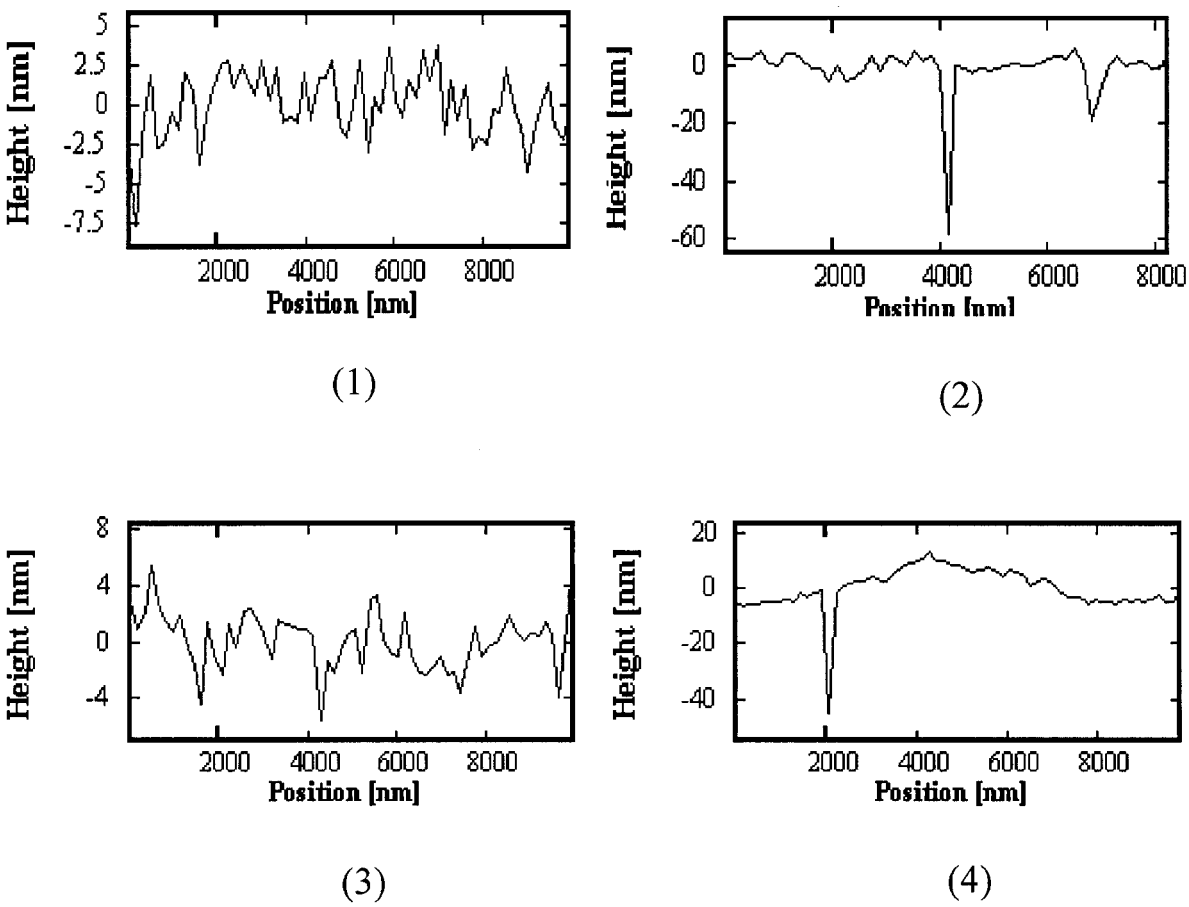

Figure 6 Representative line scans taken from different sections of the AFM image of polyaniline (EB) films. The numbers correspond to the topographical image in Figure 5.

nitrogen atmosphere for 1 h at 150°C could be recovered by redoping using a film immersion process. However, when our *UDA* films were redoped by immersing the films in a 1 M hydrochloric acid solution for 48 h, the electrical conductivity of the *UDAR* films was only 0.008 ± 0.001 S/cm (5.6%). The partial recovery in our *UDAR* films, which was less than expected, may be due to some cross-linking in the polyaniline (EB) chains that reduced the number of quinoid rings, which are essential for doping. Also, removal of the solvent during the annealing process may cause the polymer chains to become more compact, which may also reduce the number of sites accessible for doping. However, because we did not see any change in the ratio of intensities of the peaks at ~ 1530 and ~ 1615 cm^{-1} for the *UDA* films (curve '3'), we believe that the partial recovery is most likely due to the reduced accessibility of sites in the polymer chain for doping.

The electrical conductivity of the films that were annealed directly after casting and then doped, *UAD*, was 0.017 ± 0.001 S/cm (11.8%). Though the reason for annealing the films at 180°C was to avoid cross-linking in the polymer, the FTIR spectra and electrical conductivity experiments showed that there may be some initial cross-linking upon annealing, and hence fewer doping sites are present. The FTIR spectrum of the *UA* film (shown as curve '4' in Figure 4) indicates that there are a significant number of quinoid rings present in the polymer chain that can act as sites for doping. This result is confirmed by the fact that the electrical conductivity of the *UAD* film is 11.8% of the *UD* film that was made by doping the films immediately after casting.

As discussed earlier, the interfacial roughness of the polymer films plays a critical role in the properties of heterojunction diodes or any other organic microelectronic device.[9,11,31] Topographical images of the films and the corresponding linescans that are typical of the films are shown in Figures 5 and 6, respectively.

Table II Root Mean Square (rms) Roughness of the Polyaniline (EB) Films Processed under Different Conditions

Film #	EB Films after Various Processing Steps[a]	rms Roughness (nm)	% Increase in rms Roughness
1	*U*	2.86	—
2	*UD* (doped by film immersion technique with 1 M HCl for 48 h at room temperature)	4.18	46.2
3	*UDA* (annealed at 180°C for 3 h under nitrogen atmosphere)	2.78	(2.8) (decrease)
4	*UA* (annealed at 180°C for 3 h under nitrogen atmosphere)	4.01	40.2

[a] The films used in this study were 53.9 ± 3.8 μm thick, and the percent increase in rms roughness is relative to the *U* **film.**

As shown in Table II, the rms roughness of the *U* polyaniline (EB) films was 2.86 nm. On doping the EB films (*UD*), the rms roughness increased by 46.2% to 4.18 nm. These *UD* polyaniline (EB) films also showed defects, such as microvoids and pin holes, which lead to a higher surface roughness. A linescan image showing the microvoids and pin holes in the *UD* films sample (in Figure 5.2) is shown in Figure 6.2. Wen et al.[32] also observed defects, such as the formation of fibril-like structures, on doping polyaniline membranes. After annealing our doped films (to make the *UDA* films) at 180°C under a nitrogen atmosphere for 3 h, the measured rms roughness was reduced by 2.8% (to 2.78 nm) compared with the initial *U* films. When the *U* films were annealed under the same conditions, the rms roughness of these films (*UA*) increased 40.2% to 4.01 nm. The reasons for the reduction of the roughness in going from the *U* polyaniline (EB) films to *UDA* film and the increase in roughness in going from the *U* films to the *UA* films are not well understood at this stage.

In related work on free-standing polyaniline (EB) films cast by NMP, Milton and Monkman[33] reported that their *U* polyaniline (EB) films showed a decrease in roughness when annealed (to make *UA* films). To explain this result, they suggested that the removal of NMP molecules by evaporation resulted in spaces and voids ("free volume") being produced in the films. When the polyaniline (EB) films were heated beyond their glass transition temperature (T_g) of 180°C, the samples hardened. This hardening of their *UA* polyaniline (EB) film was confirmed by dynamic mechanical thermal analysis (DMTA), and they suggested that this hardening was because of a reduction in free volume due to compaction. As a result of this compaction, they proposed that the polymer chains became physically entangled. Therefore, it might be expected that any defects, such as nano-voids and micro-voids, formed on evaporation of solvent would become occupied by the polyaniline (EB) chains. Hence, their explanation suggests that the rms roughness measured on molecular length scales should show a decrease in going from a *U* film to a *UA* polyaniline (EB) film, which agrees with their experimental results.

However, in going from the *U* polyaniline (EB) film to the *UA* film, we observed that the rms roughness of the EB films increased by ~ 40%. Therefore, our findings on the effect of annealing on surface roughness of undoped, free-standing EB films appears to be contrary to what would be expected based on the observations of Milton and Monkman.[33] At this stage we are not certain why the rms roughness of the doped films reduces after thermal treatment. This phenomenon is a subject of current investigation. Nevertheless, it is important to note that the rms roughness of the *UD* films was 4.18 nm and it reduces to 2.78 nm when annealed (*UDA*), which is beneficial for creating more uniform interfaces between the polymer layer and metal contact of a device. This reduction of surface roughness should also improve the performance of the device.

CONCLUSIONS

The morphology and surface roughness of polyaniline (EB) films depend on its thermal treatment. AFM characterization of the films showed that the rms roughness of the films increased by

$\sim$ 46% after doping ($U \rightarrow UD$). However, thermal treatment of the doped films under a nitrogen atmosphere at 180°C for 3 h reduced the rms roughness to the level of the initial, undoped film ($UD \rightarrow UDA$). In another processing sequence in which the polyaniline (EB) films were annealed after being cast ($U \rightarrow UA$), the rms roughness increased by $\sim$ 40%. The electrical conductivity of these films is also strongly dependent of processing sequence. No electrical conductivity was observed in the doped polyaniline (EB) films that were subsequently annealed (*UDA* films). After redoping these thermally treated films ($UDA \rightarrow UDAR$), $\sim$ 6% of the initial conductivity could be recovered. On the other hand, the electrical conductivity of the *UAD* films was only 12% relative to the *UD* films.

The results from our AFM and doping studies indicate that one approach to lowering the roughness of polyaniline may be to anneal the doped films and then redope the film prior to making a device. However, the films should be annealed at a lower temperature (e.g., 120°C) to reduce the loss of electrical conductivity that occurs during annealing at higher temperatures (e.g., 180°C). Effective processing strategies for making polyaniline (EB) films with significantly lower rms roughness should result in improved performance of conducting polymer-based electronic devices made from these materials.

We gratefully acknowledge financial support from the Department of Chemical Engineering and the NSF Center for Advanced Engineering Fibers and Films at Clemson University (Award number EEC-9731680), and the National Textiles Center (Department of Commerce). We thank Dr. R. W. Schwartz and H. Dobberstien for use of the annealing facilities in the Department of Ceramic Engineering and K. Ivey for assistance with the DSC, TGA, and FTIR measurements. Also, we acknowledge, with thanks, Dr. T. Hanks and Dr. B. Bergman of Furman University for assistance with AFM characterization work. We also thank Dr. X. Wang, K. Eaiprasertsak, K. E. Harrison, A. M. Forster, and N. C. Gallego for helpful discussions.

REFERENCES

1. Bao, Z.; Feng, Y.; Dodabalapur, A.; Raju, V. R.; Lovinger, A. J. Chem Mater 1997, 9, 1299.
2. Rogers, J. A.; Bao, Z.; Makhija, A.; Braun, P. Adv Mater 1999, 11, 741.
3. Ebisawa, F.; Kurokawa, T.; Nara, S. J Appl Phys 1983, 54, 3255.
4. Brown, R.; Jarrett, C. P.; de Leeuw, D. M.; Matters, M. Synth Met 1997, 88, 37.
5. Horowitz, G. Adv Mater 1998, 10, 365.
6. Ridley, B. A.; Nivi, B.; Jacobson, J. M. Science 1999, 286, 746.
7. Gazotti, W. A.; Nogueria, A. F.; Girotto, E. M.; Gallazzi, M. C.; De Paoli, M.-A. Synth Met 2000, 108, 151.
8. Wen, W.; Jou, J.; Wu, H.; Cheng, C. Macromolecules 1998, 31, 6515.
9. Mazzoni, G.; Lacaita, A. L.; Perron, L. M.; Pirovano, A. IEEE Trans Electron Devices 1999, 46, 1423.
10. Chen, S.; Fang, Y. Synth Met 1993, 60, 215.
11. Bandyopadhyay, S.; Bhattacharyya, A.; Sen, S. K. J Appl Phys 1999, 85, 3671.
12. Kuo, C.; Chen, S.; Hwang, G.; Kuo, H. Synth Met 1998, 93, 155.
13. de Leeuw, D. M.; Simenon, M. M. J.; Brown, A. R.; Einerhand, R. E. F. Synth Met 1997, 87, 53.
14. Paloheimo, J.; Stubb, S. Synth Met 1997, 89, 51.
15. Abell, L.; Pomfret, S. J.; Adams, P. N.; Monkman, A. P. Synth Met 1997, 84, 127.
16. Ding, L.; Wang, X.; Gregory, R. V. Synth Met 1999, 104, 73.
17. Narasimhan, M.; Hagler, M.; Cammarata, V.; Thakur, M. Appl Phys Lett 1998, 72, 1063.
18. Paul, R. K.; Vijayanathan, V.; Pillai, C. K. S. Synth Met 1999, 104, 189.
19. Rannou, P.; Nechtschein, M. Synth Met 1997, 84, 755.
20. Sakkopoulos, S.; Vitoratos, E.; Dalas, E. Synth Met 1998, 92, 63.
21. Wei, Y.; Jang, G-W.; Hsueh, K. F.; Scherr, E. M.; MacDiarmid, A. G.; Epstein, A. J. Polymer 1992, 33, 314.
22. Kuo, C.; Chiou, W.-H. Synth Met 1997, 88, 23.
23. Tang, J.; Jing, X.; Wang, B.; Wang, F. Synth Met 1988, 24, 231.
24. Yin, W.; Ruckenstein, E. Synth Met 2000, 108, 39.
25. Angelopoulos, M.; Dipietro, R.; Zheng, W. G.; MacDiarmid, A. G.; Epstein, A. J. Synth Met 1997, 84, 35.
26. Cao, Y.; Li, S.; Xu, Z.; Guo, D. Synth Met 1986, 16, 305.
27. Kim, S.; Chung, I. J. Synth Met 1998, 97, 127.
28. Bao, Z. X.; Liu, C. X.; Kahol, P. K.; Pinto, N. J. Synth Met 1999, 106, 107.
29. Kuo, C.; Chen, C. Synth Met 1999, 99, 163.
30. Ansari, R.; Price, W. E.; Wallace, G. G. Polymer 1996, 37, 917.
31. Singh, R.; Parihar, V.; Chen, Y.; Poole, S. V.; Nimmagadda, S. V.; Vedula, L. IEEE Trans Semiconduct Manufact 1999, 12, 36.
32. Wen, L.; Kocherginsky, N. M. Synth Met 1999, 106, 19.
33. Milton, A. J.; Monkman, A. P. J Phys D: Appl Phys 1993, 26, 1468.